

On the linear stability of microtearing modes in low collisionality regimes

I. Predebon, F. Sattin

Consorzio RFX, Associazione Euratom-ENEA sulla fusione, Padova, Italy

Introduction

Microtearing modes (MTs) are short-wavelength drift-tearing modes driven by electron temperature gradients [1, 2], studied since the 1970s for their potential relevance in the electron heat transport. One of the first, most widely known and apparently well established conclusions about MTs concerns their linear stability under effectively collisionless conditions [2, 3]. Since fusion plasmas are increasingly hot and therefore less collisional, this claim caused a lessened interest towards these instabilities as relevant source of turbulence. Nonetheless, several investigations in different fusion plasmas using different gyrokinetic codes have recently gathered evidences which are partially adverse to this claim [4, 5]. However, no recent investigation appears to have faced explicitly the destabilization of MTs in collisionless regimes. This work aims to present a first step in this direction. We present a numerical analysis over a wide set of parameters, to show the existence of linear instabilities at vanishingly small collisionality. The parameters will roughly range over the reversed field pinch (RFP) experimental values. We are motivated by the reason that MTs are significantly destabilized across the electron temperature barriers occurring during the quasi-single helicity states of this configuration [6]. Two different approaches are adopted, to obtain independent results and more robust conclusions: (i) the original method described in [2], to solve the linearized drift kinetic equation together with the Ampere's law and the quasi-neutrality condition, in slab geometry; (ii) to solve linearly the gyrokinetic equation with the flux-tube code GS2, in a toroidal geometry.

Drift-kinetic approach

In the presence of a small but nonzero collisionality the relevant equations are given, e.g., in [3].

We rewrite them in a slightly different form, suitable for the forthcoming manipulations:

$$A''(x) - k_y^2 A(x) = d_A \sigma(x, \omega) (\omega A(x) - x \phi(x)) \quad (1)$$

$$\phi''(x) - k_y^2 \phi(x) = d_\phi d_A x \sigma(x, \omega) (\omega A(x) - x \phi(x)) \quad (2)$$

$$\sigma = \int_0^\infty ds s^4 e^{-s^2} \frac{\omega - 1 - \eta (s^2 - 3/2)}{[i\omega(v - i\omega)\alpha_1 - (xL_{nse}s)^2/3]} \quad (3)$$

$$d_A = \frac{8}{3\sqrt{3}} \left(\frac{\omega_p e \rho_i}{c} \right)^2, \quad d_\phi = \left(\frac{c_A}{c} \frac{L_n}{L_s} \right)^2, \quad L_{nse} = \frac{L_n}{L_s} \sqrt{\frac{m_i}{m_e}}, \quad \eta = \frac{L_n}{L_T} \quad (4)$$

$$\alpha_n = 1 + \frac{(xL_{nse}s)^2(n+1)^2}{(2n+1)(2n+3)} \left[\left(i\omega - \frac{v}{2}(n+1)(n+2) \right) \left(i\omega - \frac{v}{2}n(n+1) \right) \alpha_{n+1} \right]^{-1} \quad (5)$$

where A is the parallel vector potential, ϕ the rescaled scalar potential $\phi \rightarrow \phi(c/c_i)(L_n/L_s)$, ω_{pe} the electron plasma frequency, c_A the Alfvén speed, c the speed of light, L_n, L_T, L_s respectively the density, temperature and magnetic shear scale lengths, $L_u = -(d \log u/dr)^{-1}$; c_i, ρ_i, m_i, m_e respectively the ion thermal speed, Larmor radius, mass, and the electron mass; ω, ν are the eigenfrequency of the mode and the thermal collision frequency; k_y the mode wavenumber orthogonal to the equilibrium magnetic field and x the radial-like coordinate. Frequencies are normalized to the diamagnetic frequency ω_* , lengths to ρ_i . The condition $T_e = T_i$ is assumed. The above equations are an eigenvalue problem, with ω complex eigenvalue to be determined. Preliminarily to any new investigation we checked that our solver of the above equations reproduces the results of [2] under the same plasma conditions. Since these studies rule out positive growth rates when $\nu \ll 1$, in order to recover instability either (I) new parameter regimes must be investigated, or (II) physical mechanisms previously unaccounted for must be added.

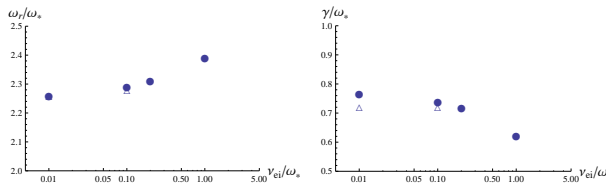


Figure 1: Real frequency ω_r and growth rate γ vs. ν . Other parameters are $k_y = 0.05$, $\beta = 0.01$, $\eta = 6$. As a convergence check, we varied the number of terms retained in the expression for α (Eq. 5): solid dots for $N = 11$ terms; open triangles for $N = 21$.

original studies. In order to further reduce the degrees of freedom here we set $L_n/L_s = \eta$.

Let us now address point (II). Any inhomogeneity of the magnetic field causes additional particle drifts. Within a slab geometry, the ∇B effect can be included in the linearized drift-kinetic equation (Eq. 1 of [2]) and appears as an additional $k_y u_d$ term: neglecting entirely collisionality $\nu = 0$ one writes

$$i(\omega - k_{\parallel} u_{\parallel} - k_y u_d) \tilde{f} = e/TE_{\parallel} v_{\parallel} f_{eq} -$$

$(ik_y c/B)(\phi - Av_{\parallel}/c)(\partial f_{eq}/\partial x)$, where \tilde{f} is the perturbed electron distribution, f_{eq} the Maxwellian equilibrium distribution, $E_{\parallel} = i\omega/cA - ik_{\parallel}\phi$, $k_{\parallel} = k_y x/L_s$. The precise expression

Concerning point (I): in present-days RFPs particle fuelling is commonly provided through recycling from the wall; accordingly, density profiles are quite flat and the density length scale L_n rather large. Conversely, internal heat transport barriers are commonly encountered, thus L_T can be locally fairly small. Finally, L_s , in a RFP, is of the order of the minor radius a . We are thus going to study the case $\eta, L_n/L_s > 1$ that was not addressed in

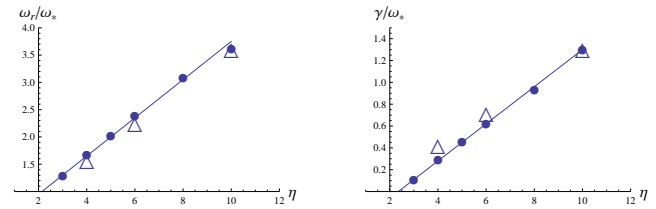


Figure 2: Real frequency ω_r and growth rate γ vs. η . Dots are for $\nu = 1$, triangles for $\nu = 0.01$. Other parameters are $k_y = 0.05$, $\beta = 0.01$.

for the drift velocity u_d depends on the geometry of the magnetic field. Since we are interested in qualitative results, a dimensional analysis shows that it can be written as $u_d = \epsilon L_n / L_s$ (in units $\rho_i \omega_\star$), with ϵ a dimensionless parameter of order unity.

The solution \tilde{f} is used to compute the perturbed current density, to be inserted into the Ampere's law.

In the presence of large η and vanishingly small ν the conductivity σ shrinks to a very narrow layer around $x = 0$, of width roughly the electron Larmor radius. It appears therefore reasonable in this case to neglect the electrostatic potential ϕ , that by symmetry vanishes at $x = 0$, and use just Ampere law to compute ω .

Results for hypotheses (I) and (II) are summarized in Figs. 1–3. The conclusion is that instability can be found in both regimes.

Gyrokinetic approach

The gyrokinetic equation is solved in a flux tube domain by means of the electromagnetic code GS2, adapted to the RFP geometry [8]. The RFP geometry is characterized by a large poloidal component of the magnetic field, with $q \ll 1$ everywhere, $q < 0$ in the very edge and $q \sim 0.1$ at mid-radius with magnetic shear $\hat{s} \sim -1$. The peculiar terms of the RFP geometry are the ∇B and curvature drifts in the drift frequency, say $\omega_{\nabla B}$ and ω_k , which include terms proportional to B_θ^2/ρ and $-\partial B/\partial \rho$ respectively; the parallel gradient is $\mathbf{b} \cdot \nabla \propto (B_\theta/\rho)\partial_\theta$; the binormal wavenumber k_y has a ϕ component largely dominant over the θ component in the plasma edge.

In order to have eigenmodes sufficiently resolved, the longitudinal grid is extended to the interval $\theta \in [-32\pi, 32\pi]$. Fluctuations in ϕ and A_{\parallel} are considered. Plasmas with two species only, main ions and electron, are analyzed. We start from a typical quasi-single helicity case, but with a much higher β , so as to get relevant growth rates in a large range of collisionality.

We show in Fig. 4 the growth rate of the fastest growing (MT) mode for a flat-density high-beta plasma. We have defined $\epsilon_{\nabla B}, \epsilon_k \in [0, 1]$ as parameters weighting the fraction of $\omega_{\nabla B}$ and

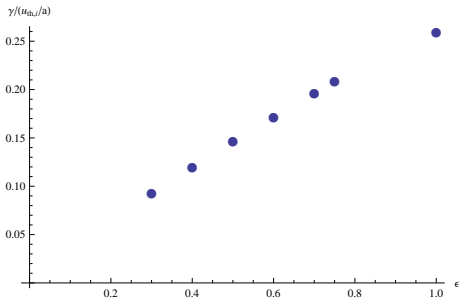


Figure 3: Growth rate vs. ϵ , which quantifies the amount of grad-B drift. Other parameters are $k_y = 0.15$, $\eta = 20$, $L_n/L_s = 24$. The growth rate is normalized to c_s/a (ion sound speed over minor radius).

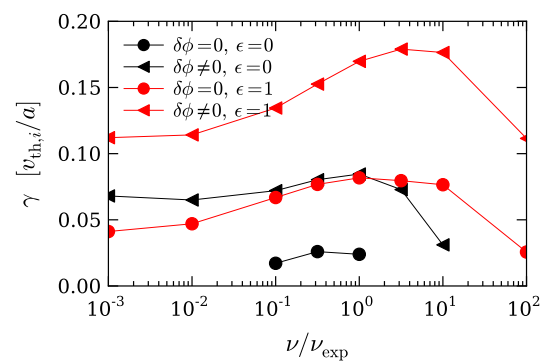


Figure 4: Growth rate vs. collisionality, w/wo electrostatic fluctuations, w/wo $\omega_{\nabla B}$ and ω_k drifts. Relevant parameters: $a/L_{T_e} = 4$, $a/L_n = 0$, $\hat{s} = -0.65$, $q = 0.12$, $\beta_e = 0.05$, $k_y = 0.1$.

ω_k , respectively, keeping $\varepsilon_{\nabla B} = \varepsilon_k \equiv \varepsilon$ at the moment. While the curves have a maximum for $v \sim v_{\text{exp}}$, the growth rate is non-vanishing also for $v/v_{\text{exp}} \ll 1$, except for the case with $\delta\phi = 0$ and $\varepsilon = 0$ ($\delta\phi \neq 0$ is always destabilizing, cf. [9]).

Large growth rates for $\varepsilon = 1$ correspond to up-shifted $\gamma(k_y)$ spectra, peaked in the interval $0.5 < k_y < 1.0$. It is interesting to quantify how the single drifts separately modify the destabilization of MTs, Fig. 5. The study is performed with $\delta\phi \neq 0$, at a higher wavenumber and β , and much lower collisionality, $v/v_{\text{exp}} = 10^{-6}$. For $\varepsilon_{\nabla B} = 0 = \varepsilon_k$ MTs are stable, at this wavenumber. As already shown above, high ∇B and curvature drifts are not the only destabilizing mechanism at low collisionality. In Fig. 6 we show the growth rate as a function of both the magnetic shear \hat{s} and the logarithmic density gradient a/L_n for a low collisionality plasma, $v/v_{\text{exp}} = 10^{-3}$, and with $\varepsilon_{\nabla B} = 0 = \varepsilon_k$. Furthermore, the trapped particle fraction is set to 0, so as to exclude that contribution. As is shown, the growth rate is getting larger for increasing L_n/L_s , being $L_s^{-1} \propto \hat{s}$. The same scan performed setting $\delta\phi = 0$ provides MT stability for every $(a/L_n, \hat{s})$.

Conclusions

Summarizing, we have presented some parametric studies, showing that MTs can be destabilized even in collisionless regimes under certain conditions and geometries of the plasma. Extended results will be discussed in a separate paper.

References

- [1] R. D. Hazeltine *et al.*, Phys. Fluids **18**, 1778 (1975).
- [2] J. F. Drake *et al.*, Phys. Rev. Lett. **44**, 994 (1980).
- [3] N. T. Gladd *et al.* Phys. Fluids **23**, 1182 (1980).
- [4] H. Doerk *et al.* Phys. Plasmas **19** 055907 (2012).
- [5] F. Sattin *et al.* 15th International RFP workshop (2011), pdf.
- [6] I. Predebon *et al.*, Phys. Rev. Lett. **105**, 195001 (2010).
- [7] <http://gs2.sourceforge.net>
- [8] I. Predebon *et al.*, Phys. Plasmas **17**, 012304 (2010).
- [9] D. J. Applegate *et al.*, Plasma Phys. Control. Fusion. **49** 1113 (2007).

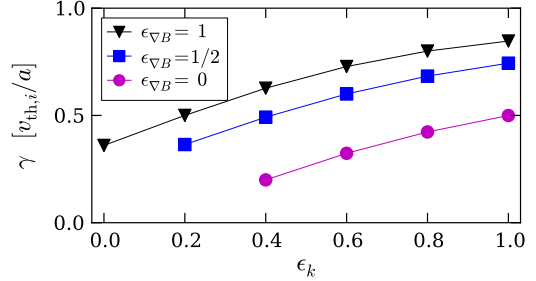


Figure 5: Growth rate as a function of fractions of $\omega_{\nabla B}$ and ω_k . Relevant parameters: $a/L_{T_e} = 4$, $a/L_n = 0.2$, $\hat{s} = -0.65$, $q = 0.12$, $\beta_e = 0.08$, $k_y = 0.5$.

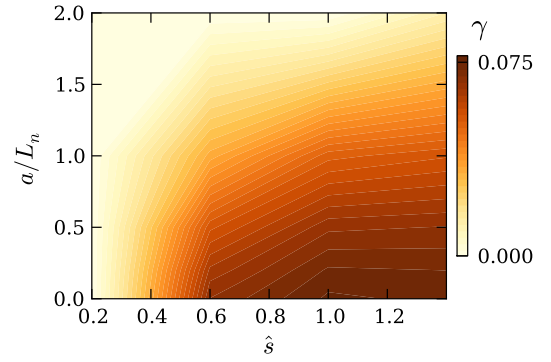


Figure 6: Growth rate vs. magnetic shear and density gradient, with $\delta\phi \neq 0$. Relevant parameters: $a/L_{T_e} = 6$, $q = 0.12$, $\beta_e = 0.05$, $v/v_{\text{exp}} = 10^{-3}$, $\varepsilon_{\nabla B} = 0 = \varepsilon_k$, $k_y = 0.1$.